Pacific Northwest
NATIONAL LABORATORY

PNNL-34996

A Multifidelity and Multimodal Machine Learning Approach for Extracting Bonding Environments of Impurities and Dopants from X-ray Spectroscopies

September 2023

Micah P Prange
Niranjan Govind
Panos Stinis
Eugene S Ilton
Amanda A Howard

U.S. DEPARTMENT OF ENERGY

Prepared for the U.S. Department of Energy
under Contract DE-AC05-76RL01830

DISCLAIMER

PACIFIC NORTHWEST NATIONAL LABORATORY
operated by
BATTELLE
for the
UNITED STATES DEPARTMENT OF ENERGY
under Contract DE-AC05-76RL01830

Printed in the United States of America

Available to DOE and DOE contractors from
the Office of Scientific and Technical Information,
P.O. Box 62, Oak Ridge, TN 37831-0062
www.osti.gov
ph: (865) 576-8401
fox: (865) 576-5728
email: reports@osti.gov

Available to the public from the National Technical Information Service
5301 Shawnee Rd., Alexandria, VA 22312
ph: (800) 553-NTIS (6847)
or (703) 605-6000
email: info@ntis.gov
Online ordering: http://www.ntis.gov

PNNL-34996

A Multifidelity and Multimodal Machine Learning Approach for Extracting Bonding Environments of Impurities and Dopants from X-ray Spectroscopies

September 2023

Micah P Prange
Niranjan Govind
Panos Stinis
Eugene S Ilton
Amanda A Howard

Prepared for
the U.S. Department of Energy
under Contract DE-AC05-76RL01830

Pacific Northwest National Laboratory
Richland, Washington 99354

Abstract

Extended X-ray absorption fine structure (EXAFS) spectroscopy is crucial for determining the coordination environment of impurities and dopants; however, it requires difficult measurements. X-ray absorption near edge structure (XANES) spectroscopy and X-ray emission spectroscopy (XES) can be obtained easily but cannot be converted to determine structures. In this work we develop tools to map measured XANES to the EXAFS signal through machine learning, thereby facilitating the use of EXAFS structural-determination analyses on XANES data. Through the use of Deep Operator Networks (DeepONets), we are able to accurately predict the EXAFS spectrum between 6 and 14 $Å^{-1}$ from the first 6 $Å^{-1}$ (~100 eV) of the absorption spectrum of Cu^{2+} substitutional defects in the Fe^{3+} mineral hematite ($\alpha - Fe_2O_3$). This surprising finding implies that theoretical analyses of X-ray absorption spectra could be implemented that extract the *same* conclusions as high-quality EXAFS studies from spectra collected over a much smaller range of photon energies. To encourage similar efforts, the simulated x-ray spectra, machine learning, and fitting code is made publicly available.

Acknowledgments

This research was supported by the **Physical and ComputationalSciences Division Mission Seed** under the Laboratory Directed Research and Development (LDRD) Program at Pacific Northwest National Laboratory (PNNL). PNNL is a multi-program national laboratory operated for the U.S. Department of Energy (DOE) by Battelle Memorial Institute under Contract No. DE-AC05-76RL01830.

Acronyms and Abbreviations

AIMD: Ab initio molecular dynamics
DNN: Deep neural network
DeepONet: Deep Operator Network
EXAFS: Extended x-ray absorption fine structure
FFT: Fast Fourier transform
NN: Neural network
XANES: X-ray absorption near edge

Contents

Figures

Tables

1.0 Introduction

This work involves relating two different types of x-ray absorption spectra: x-ray absorption near edge structure (XANES) and extended x-ray absorption fine structure (EXAFS) (Sayers, Lytle, and Stern 1969), which are conventionally used to probe the local electronic and atomic structures, respectively, of a specific chemical element in a sample. The experimental accessibility of the two types of spectral data is different: XANES can be measured on more dilute samples and with less stringent requirements on the x-ray source and detector. Hence it is of interest to understand the relationship between EXAFS and XANES. Machine learning has proven useful for uncovering subtle relationships that are not apparent using traditional analysis. In this work we demonstrate that, in a certain class of simulated data, machine learning can predict the EXAFS of a sample when shown only the XANES and not the atomic structure that would normally be used to simulate the EXAFS. This finding suggests that it may be possible to extend experimentally measured XANES spectra to the EXAFS and thereby increase the conditions under which EXAFS can be obtained. We achieved this using the DeepONet framework (Lu et al. 2021), which is part of body of work for operator learning (Lu et al. 2022; Li et al. 2020a; 2020b; You et al. 2022) inspired by the universal approximation theorem for operators (Chen and Chen 1995; Back and Chen 2002). DeepONets have been shown to accurately predict a wide range of physical systems (Sharma Priyadarshini, Venturi, and Panesi 2021; Ranade, Gitushi, and Echekki 2021; 2021; Di Leoni et al. 2021; He et al. 2023; Goswami et al. 2022; 2023; Lin et al. 2021). In this report we summarize our main findings, showing that DeepONets can accurately predict EXAFS profiles from corresponding XANES profiles.

2.0 DeepONets to predict EXAFS from XANES

2.1 Synthetic XAS Spectra

We conducted this research using ab initio molecular dynamics (AIMD) from our previous work (Mergelsberg et al. 2021) that describe Cu bearing hematite, a naturally occurring mineral. We used the FEFF code (Kas et al. 2021) to simulate both XANES and EXAFS for many instantaneous structures form the AIMD simulations. Key settings were kept fixed for all runs: $R_{max} = 9$ Å, $R_{FMS} = 8.5$ Å and $l_{max} = 3$.

2.2 DeepONets

The primary objective of this work was to train a machine learning surrogate model to find the mapping from the space a XANES profiles generated by the training set to the space of EXAFS profiles. Through testing, we found success using a variation of DeepONets (Lu et al. 2021) called the modified DeepONet (Wang, Wang, and Perdikaris 2021). A DeepONet has two deep neural networks, which take as input the XANES profile to the branch net and the independent variables, typically spatial coordinates, to the trunk net. The branch and trunk net are combined with a dot product to give the output, in this case a prediction of the EXAFS profile. In modified DeepONets, encoder layers are added to enable more communication between the input variables, in the form of a convex combination at each hidden layer of the branch and trunk DNNs.

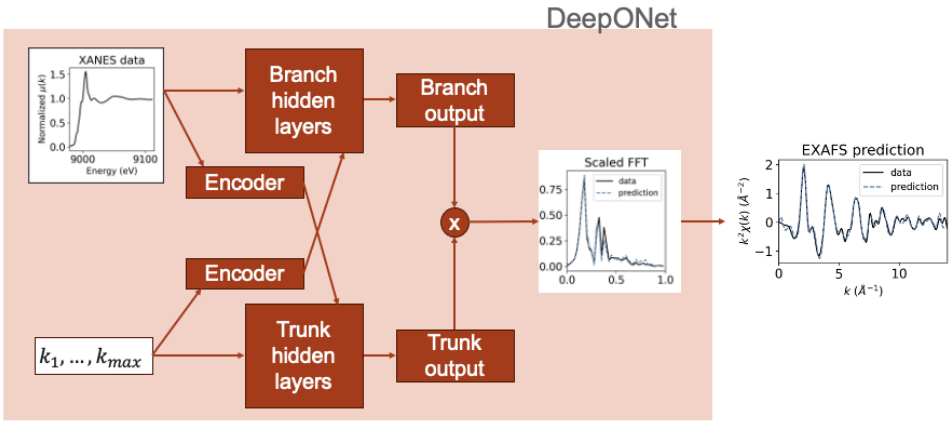

Figure 1: Diagram of the DeepONet

Through trial, we found that the modified DeepONet surrogate model produces more robust and accurate results if instead of training for the EXAFS profile directly, we instead learn the Fourier transform of the EXAFS with respect to k. In this variation, the trunk network takes as input the k grid of the Fourier transform, and the output of the modified DeepONet is the Fourier transform of the EXAFS corresponding to XANES profile used as input to the branch network. A diagram of the training process is given in Figure 1.

We generated training and testing sets from snapshots from ab initio molecular dynamics (AIMD) simulations. Because the ultimate use case for this work consists of identifying linear combinations of given configurations, we also included linear combinations of the snapshots from the AIMD simulations. Additionally, we included the averages of all the snapshots from a given simulation, and linear combinations of those averages. The training set consisted of data from 10 configurations, and three configurations were withheld to comprise the test set. This resulted in a total training set size of 2349, consisting of 10 averages of all snapshots for a given configuration, 1000 linear combinations of the averaged profiles, 339 unaveraged snapshots, and 1000 linear combinations of the unaveraged snapshots. The testing set had total size 235, consisting of 3 averages of all snapshots for a given configuration, 21 linear combinations of the averaged profiles, 111 unaveraged snapshots, and 100 linear combinations of the unaveraged snapshots. To improve training, each type of data was assigned a weight w, which was included in the lost function to assign higher weight to the averaged profiles. The weights used were 3 for the averaged profiles and linear combinations of averaged profiles, 2 for linear combinations of snapshots, and 1 for the snapshots.

The output of the DeepONet is denoted by $\mathcal{N}\left(X_i(k_j;\theta)\right)$, where θ is the set of all trainable parameters, k_j is a given Fourier coordinate, and X_i is the EXAFS profile for sample *i*. The goal in training is to minimize the loss function, given by

$$\mathcal{L}(\theta) = \frac{1}{N_b}\frac{1}{k_{max}}\sum_{i=1}^{N_b}\sum_{j=1}^{k_{max}} w_i^2\left[\left(\Re\left[\mathcal{N}\left(X_i(k_j;\theta)\right)\right]-\Re[X_i(k_j)]\right)^2+\left(\Im\left[\mathcal{N}\left(X_i(k_j;\theta)\right)\right]-\Im[X_i(k_j)]\right)^2 + \left(\left|\mathcal{N}\left(X_i(k_j;\theta)\right)\right|^2-\left|X_i(k_j)\right|^2\right)^2\right]$$

The loss function contains terms for the mean squared error (MSE) for the real part of the Fourier transform, the imaginary part of the Fourier transform, and the magnitude of the Fourier transform.

The DeepONet is implemented in Jax (Bradbury et al. 2018), and all training parameters are given in Table 1.

Table 1: Hyperparameters for training the DeepONet

Training parameter	Value
Number of Fourier coefficients	k_{max} =40
FFT input scaling	4/282
FFT coordinate scaling	1/40
XANES shift	-1
DNN network size	6 hidden layers, 200 neurons each
Number of training iterations	600,000
Learning rate	`exponential_decay` function in Jax with initial learning rate 5×10^{-5} and 2000 decay steps with a decay rate of 0.99
Activation function	scaled exponential linear unit (SELU)
XANES data used in training	$k \in [0, 6]$ (Å^{-1})

To calculate the accuracy of the trained DeepONet surrogate, we calculated the relative l_2 error, given by

$$Error = \frac{\|\chi_{DoN}(k) - \chi_{FEFF}(k)\|_2}{\|\chi_{FEFF}(k)\|_2}$$

where $\|\cdot\|_2$ denotes the l_2 norm, and $\chi_{FEFF}(k)$ and $\chi_{DoN}(k)$ are the FEFF and DeepONet EXAFS spectra, respectively. Note that the error is calculated as a post processing step, after the inverse Fourier transform is taken. The mean relative l_2 error from our trained DeepONet model is 0.176, calculated over the full test set. When calculated only over averaged profiles and linear combinations of averages, the mean relative l_2 error is 0.163. The results represent accurate predictions of EXAFS profiles that can accurately be used in further work where EXAFS profiles are needed, without the need to do costly experiments to find the EXAFS profile. Example profiles generated by training are given in Figure 2 for the three averaged profiles in the test set.

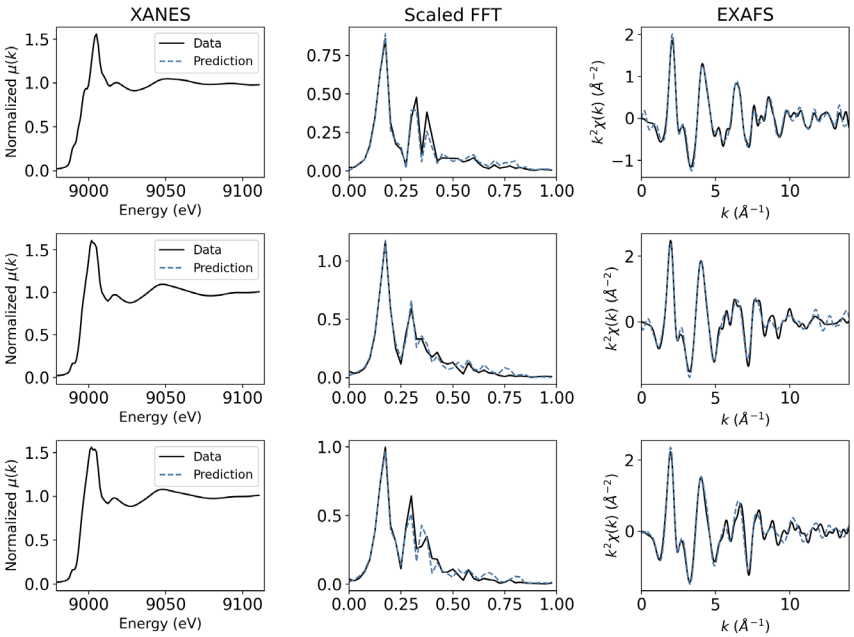

Figure 22: DeepONet predictions for the three profiles of averaged snapshots in the training set. From left to right we plot the input XANES profile, the scaled FFT values, and the predicted, unscaled, EXAFS profiles.

3.0 Conclusions

We have shown that DeepONets can be trained to predict FEFF EXAFS from FEFF XANES with high fidelity, suggesting that machine learning can be used to extend experimental XANES spectra to include the EXAFS region without explicit measurements. We invite others to join this effort by providing the codes used to generate the results, the trained DeepONet parameters, and simulation results used on http://datahub.pnnl.gov and https://github.com/pnnl/DeepONets_for_spectroscopy/.

4.0 References

Back, Andrew D, and Tianping Chen. 2002. “Universal Approximation of Multiple Nonlinear Operators by Neural Networks.” *Neural Computation* 14 (11): 2561–66.

Bradbury, James, Roy Frostig, Peter Hawkins, Matthew James Johnson, Chris Leary, Dougal Maclaurin, George Necula, et al. 2018. “JAX: Composable Transformations of Python+NumPy Programs.” http://github.com/google/jax.

Chen, Tianping, and Hong Chen. 1995. “Universal Approximation to Nonlinear Operators by Neural Networks with Arbitrary Activation Functions and Its Application to Dynamical Systems.” *IEEE Transactions on Neural Networks* 6 (4): 911–17.

Di Leoni, P Clark, Lu Lu, Charles Meneveau, George Karniadakis, and Tamer A Zaki. 2021. “Deeponet Prediction of Linear Instability Waves in High-Speed Boundary Layers.” *ArXiv Preprint ArXiv:2105.08697*.

Goswami, Somdatta, Ameya D Jagtap, Hessam Babaee, Bryan T Susi, and George Em Karniadakis. 2023. “Learning Stiff Chemical Kinetics Using Extended Deep Neural Operators.” *ArXiv Preprint ArXiv:2302.12645*.

Goswami, Somdatta, Minglang Yin, Yue Yu, and George Em Karniadakis. 2022. “A Physics-Informed Variational DeepONet for Predicting Crack Path in Quasi-Brittle Materials.” *Computer Methods in Applied Mechanics and Engineering* 391: 114587.

He, QiZhi, Mauro Perego, Amanda A Howard, George Em Karniadakis, and Panos Stinis. 2023. “A Hybrid Deep Neural Operator/Finite Element Method for Ice-Sheet Modeling.” *ArXiv Preprint ArXiv:2301.11402*.

Kas, J. J., F. D. Vila, C. D. Pemmaraju, T. S. Tan, and J. J. Rehr. 2021. “Advanced Calculations of X-Ray Spectroscopies with It FEFF10 and Corvus.” *Journal of Synchrotron Radiation* 28 (6): 1801–10. https://doi.org/10.1107/S1600577521008614.

Li, Zongyi, Nikola Kovachki, Kamyar Azizzadenesheli, Burigede Liu, Kaushik Bhattacharya, Andrew Stuart, and Anima Anandkumar. 2020a. “Fourier Neural Operator for Parametric Partial Differential Equations.” *ArXiv Preprint ArXiv:2010.08895*.

———. 2020b. “Neural Operator: Graph Kernel Network for Partial Differential Equations.” *ArXiv Preprint ArXiv:2003.03485*.

Lin, Chensen, Martin Maxey, Zhen Li, and George Em Karniadakis. 2021. “A Seamless Multiscale Operator Neural Network for Inferring Bubble Dynamics.” *Journal of Fluid Mechanics* 929.

Lu, Lu, Pengzhan Jin, Guofei Pang, Zhongqiang Zhang, and George Em Karniadakis. 2021. “Learning Nonlinear Operators via DeepONet Based on the Universal Approximation Theorem of Operators.” *Nature Machine Intelligence* 3 (3): 218–29.

Lu, Lu, Xuhui Meng, Shengze Cai, Zhiping Mao, Somdatta Goswami, Zhongqiang Zhang, and George Em Karniadakis. 2022. “A Comprehensive and Fair Comparison of Two Neural Operators (with Practical Extensions) Based on Fair Data.” *Computer Methods in Applied Mechanics and Engineering* 393: 114778.

Mergelsberg, Sebastian T., Micah Prange, Duo Song, Eric J. Bylaska, Sarah A. Saslow, Jeffrey G. Catalano, and Eugene S. Ilton. 2021. “Resolving Configurational Disorder for Impurities in a Low-Entropy Phase.” *The Journal of Physical Chemistry Letters* 12 (24): 5689–94. https://doi.org/10.1021/acs.jpclett.1c01218.

Ranade, Rishikesh, Kevin Gitushi, and Tarek Echekki. 2021. “Generalized Joint Probability Density Function Formulation Inturbulent Combustion Using DeepONet.” *ArXiv Preprint ArXiv:2104.01996*.

Sayers, D. E., F. W. Lytle, and E. A. Stern. 1969. “Point Scattering Theory of X-Ray K-Absorption Fine Structure.” *Advances in X-Ray Analysis* 13: 248–71. https://doi.org/10.1154/S0376030800011381.

Sharma Priyadarshini, Maitreyee, Simone Venturi, and Marcp Panesi. 2021. “Application of DeepOnet to Model Inelastic Scattering Probabilities in Air Mixtures.” In *AIAA AVIATION 2021 FORUM*, 3144.

Wang, Sifan, Hanwen Wang, and Paris Perdikaris. 2021. “Improved Architectures and Training Algorithms for Deep Operator Networks.” arXiv. http://arxiv.org/abs/2110.01654.

You, Huaiqian, Yue Yu, Marta D’Elia, Tian Gao, and Stewart Silling. 2022. “Nonlocal Kernel Network (NKN): A Stable and Resolution-Independent Deep Neural Network.” *Journal of Computational Physics* 469: 111536.

Pacific Northwest National Laboratory

902 Battelle Boulevard
P.O. Box 999
Richland, WA 99354

1-888-375-PNNL (7665)

www.pnnl.gov